A&A 429, 559–567 (2005)
DOI: 10.1051/0004-6361:20041465

Astronomy & Astrophysics

Diffuse Interstellar Bands in NGC 1448⋆,⋆⋆

J. Sollerman[1], N. Cox[2], S. Mattila[1], P. Ehrenfreund[2,3], L. Kaper[2], B. Leibundgut[4], and P. Lundqvist[1]

[1] Stockholm Observatory, Department of Astronomy, AlbaNova, 106 91 Stockholm, Sweden
e-mail: jesper@astro.su.se
[2] Astronomical Institute "Anton Pannekoek", University of Amsterdam, Kruislaan 403, 1098, The Netherlands
[3] Astrobiology Laboratory, Leiden Institute of Chemistry, PO Box 9502, 2300 RA Leiden, The Netherlands
[4] European Southern Observatory, Karl-Schwarzschild-Strasse 2, 85748 Garching, Germany

Received 14 June 2004 / Accepted 7 August 2004

Abstract. We present spectroscopic VLT/UVES observations of two emerging supernovae, the Type Ia SN 2001el and the Type II SN 2003hn, in the spiral galaxy NGC 1448. Our high resolution and high signal-to-noise spectra display atomic lines of Ca II, Na I, Ti II and K I in the host galaxy. In the line of sight towards SN 2001el, we also detect over a dozen diffuse interstellar bands (DIBs) within NGC 1448. These DIBs have strengths comparable to low reddening galactic lines of sight, albeit with some variations. In particular, a good match is found with the line of sight towards the σ type diffuse cloud (HD 144217). The DIBs towards SN 2003hn are significantly weaker, and this line of sight has also lower sodium column density. The DIB central velocities show that the DIBs towards SN 2001el are closely related to the strongest interstellar Ca II and Na I components, indicating that the DIBs are preferentially produced in the same cloud. The ratio of the λ 5797 and λ 5780 DIB strengths ($r \sim 0.14$) suggests a rather strong UV field in the DIB environment towards SN 2001el. We also note that the extinction estimates obtained from the sodium lines using multiple line fitting agree with reddening estimates based on the colors of the Type Ia SN 2001el.

Key words. supernovae: individual: SN 2001el, SN 2003hn – galaxies: individual: NGC 1448 – ISM: lines and bands – supernovae: general

1. Introduction

1.1. Extragalactic DIBs

The Diffuse Interstellar Bands (DIBs) are a large number of absorption lines between ~4000−10 000 Å that are superimposed on the interstellar extinction curve (e.g., Herbig 1995). During the last 7 decades of DIB studies almost 300 DIBs have been detected. Within the Milky Way, DIBs have been observed towards more than a hundred stars. However, there is still no definitive identification of the DIB carriers. Recent studies indicate that the environmental behaviors of DIBs reflect an interplay between ionization, recombination, dehydrogenation and destruction of chemically stable species (Herbig 1995; Cami et al. 1997; Voung & Foing 2000). It is therefore of interest to study DIBs in different environments, especially in external galaxies.

Hitherto, only a handful of DIBs have been observed in extragalactic targets (e.g., Vladilo et al. 1987; Morgan 1987; Heckman & Lehnert 2000; Ehrenfreund et al. 2002). The Magellanic Clouds have been most intensely studied in this respect. Detailed views of LMC DIBs were obtained towards the bright supernova SN 1987A (Vladilo et al. 1987). Today, high resolution spectra can also be obtained of reddened stars in the LMC with large telescopes (Ehrenfreund et al. 2002). For more distant galaxies, however, supernovae still provide the most promising opportunity to probe the extragalactic interstellar medium. Spectra taken of SN 1986G in the nearby galaxy NGC 5128 (Rich 1987; D'Odorico et al. 1989) allowed the detection of a few extragalactic DIBs outside the Local Group. Some DIBs were also tentatively detected towards SN 1989M in NGC 4579 (Steidel et al. 1990).

In this paper we present high-resolution observations of two emerging supernovae in NGC 1448. The data of the well studied Type Ia SN 2001el allowed us to detect more than a dozen extragalactic DIBs with unprecedented signal-to-noise. At a different line-of-sight through the same galaxy, the Type II SN 2003hn did not show the same spectacular DIB signal.

1.2. SNe 2001el and 2003hn in NGC 1448

Supernova 2001el was discovered on September 17.1 (UT) 2001 (Monard 2001). It was situated about 14″ West and 20″ North of the nucleus of the nearby warped spiral galaxy

⋆ Based on observations collected at the European Southern Observatory, Paranal, Chile (ESO Programmes 67.D-0227 and 71.D-0033).
⋆⋆ Table 3 and Figs. 2 and 4 are only available in electronic form at http://www.edpsciences.org

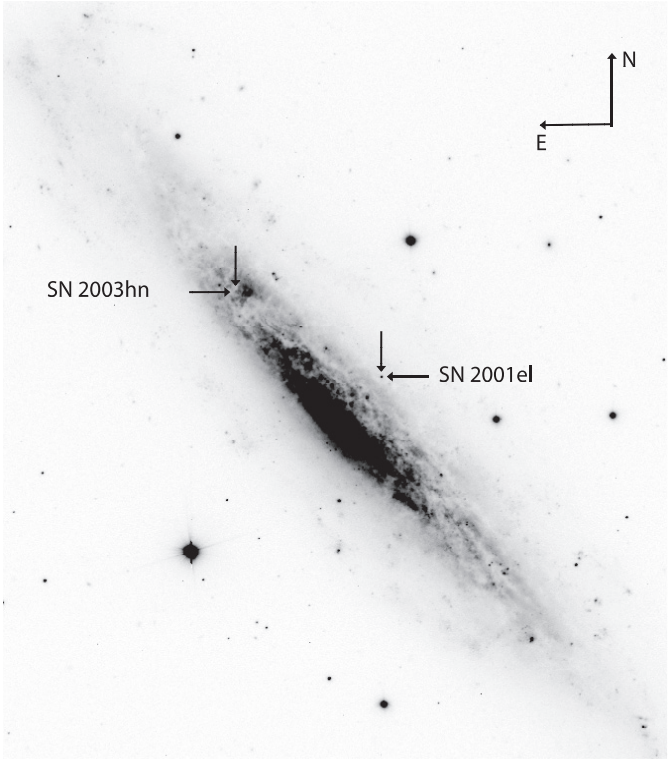

Fig. 1. Supernova 2001el as observed in the V-band with FORS1 on the VLT in August 2002, i.e., almost one year past explosion. This late image shows the position of the supernova within the galaxy NGC 1448. The field of view of the image is 4.′5 × 5.′1. North is up and East to the left. The locations of the two supernovae, SNe 2001el and 2003hn, are marked by arrows.

NGC 1448 (Fig. 1). Within our Target-of-Opportunity programme to carry out early high resolution spectroscopy of nearby supernovae (e.g., Lundqvist et al. 2004), we obtained a first spectrum on September 21. This allowed a classification of the supernova as a Type Ia observed well before maximum (Sollerman et al. 2001).

SN 2001el reached its maximum magnitude (B = 12.8 mag) on 2001 September 30, and thereby became the brightest supernova that year. This supernova has been well monitored both photometrically and spectroscopically, and has been shown to be a normal Type Ia supernova (Krisciunas et al. 2003).

SN 2003hn was discovered in the same galaxy on August 25.7 2003 (Evans 2003). It was located approximately 47″ East and 53″ North of the nucleus (Fig. 1). Spectroscopy showed this to be a Type II supernova approximately 2 weeks after explosion (Salvo et al. 2003). In this case we were motivated by our previous detection of DIBs against SN 2001el in the very same galaxy. We therefore executed high-resolution spectroscopy also for SN 2003hn, to probe the interstellar matter in another line-of-sight in NGC 1448.

In Sect. 2 we will outline the observations and data reduction procedures. The results are then presented in Sect. 3 and discussed in Sect. 4. We summarize our conclusions in Sect. 5.

Table 1. Log of VLT/UVES observations of SN 2001el.

Date (01 09)	MJD (52000+)	Exp. (s)	Airmass	Seeing[a] (arcsec)	Set-up	Slit width (arcsec)
21	173.22	2400	1.30	0.82	390+564[b]	0.8
21	173.25	2400	1.19	0.79	390+564	0.8
21	173.28	2400	1.12	0.65	437+860[c]	0.8
21	173.31	2400	1.08	0.85	437+860	0.8
26	178.36	1200	1.10	1.43	346+580[d]	0.7
26	178.39	1200	1.12	1.43	346+580	0.7
28	180.22	3000	1.20	1.05	390+564	0.8
28	180.26	3000	1.11	1.08	390+564	0.8
28	180.29	3000	1.07	1.12	390+564	0.8

[a] Seeing from the DIMM-monitor.
[b] 390+564 covers wavelength ranges 3260–4450, 4580–6680 Å.
[c] 437+860 covers wavelength ranges 3730–4990, 6600–10 600 Å.
[d] 346+580 covers wavelength ranges 3030–3880, 4760–6840 Å.

Table 2. Log of VLT/UVES observations of SN 2003hn.

Date (03 08)	MJD (52000+)	Exp. (s)	Airmass	Seeing[a] (arcsec)	Set-up	Slit width (arcsec)
31	882.26	1400	1.42	0.57	390+564[b]	0.8
31	882.28	1400	1.32	0.61	390+564	0.8
31	882.30	1400	1.25	0.52	390+564	0.8
31	882.33	1400	1.15	0.51	437+860[c]	0.8
31	882.34	1400	1.11	0.55	437+860	0.8
31	882.36	1400	1.09	0.53	437+860	0.8

[a] Seeing from the DIMM-monitor.
[b] 390+564 covers wavelength ranges 3260–4450, 4580–6680 Å.
[c] 437+860 covers wavelength ranges 3730–4990, 6600–10 600 Å.

2. Observations and data reduction

All observations were obtained with the Ultraviolet and Visual Echelle Spectrograph (UVES)[1] on the second unit telescope (Kueyen) of the Very Large Telescope (VLT) on Paranal, Chile. UVES is a high-resolution two-arm cross-dispersed Echelle spectrograph, where both arms can be operated simultaneously using a dichroic beamsplitter (Kaufer et al. 2002). This enables high efficiency from the atmospheric cutoff in the blue to the long-wavelength limit of the CCDs in the red.

On the night of September 21, we obtained 4 exposures of 2400 s each of SN 2001el. These were divided into two set-ups, in order to obtain a complete wavelength coverage. The log of all our observations of SN 2001el is given in Table 1. The supernova was observed again on September 26 and was revisited for the last time on September 28. The observations were thus obtained 9, 4 and 2 days before maximum light of the supernova.

The observations of SN 2003hn were obtained on August 31, 2003. We obtained 3 exposures of 1400 s each in both the red and blue set-ups. The details are given in Table 2. This supernova was only observed once, and since it was also

[1] www.eso.org/instruments/UVES/

at least one magnitude fainter than SN 2001el at the time of our observations, the signal-to-noise of the SN 2003hn data is not as good as for SN 2001el.

The spectra were interactively reduced using the UVES-pipeline[2] as implemented in `MIDAS`. This reduction package allows for bias subtraction and flat-fielding of the data using calibration frames obtained in the morning. Wavelength calibration can be very accurately achieved by comparison to ThAr arc lamps.

In searching for the DIBs, we summed together all the observations from epochs 1 and 3 for SN 2001el, when applicable (see Table 1). The second epoch was not added to the final spectrum, since the exposure time was shorter and the seeing was worse at this epoch. For SN 2003hn all available data were combined.

3. Results

3.1. Interstellar atomic lines

Superposed on the spectra of SNe 2001el and 2003hn we detect interstellar atomic absorption lines, both from the Milky Way (MW; $l = 251.5°$, $b = -51.4°$) and from NGC 1448. The detected lines are Ca II K & H (3933.66, 3968.47 Å), Na I D (5889.95, 5895.92 Å) and Ti II (3383.76 Å). K I (7664.90, 7698.96 Å) was also detected for SN 2001el, albeit with much weaker signal. The strongest components of these lines come from absorption within NGC 1448 (see Table 3).

The Ca II H & K lines are clearly detected also in the MW. On the sky, the two lines-of-sight given by the two supernovae are separated by about 69 arcsec. The MW line profiles also look very similar with two strong components centered at heliocentric radial velocities of about 10 to 20 km s^{-1} (Fig. 2; Table 3). Towards SN 2001el we also detect a high velocity component at ∼158 km s^{-1} which can not be seen in the noisier data obtained towards SN 2003hn.

For the NGC 1448 components of Ca II H & K, the differences between the two lines of sight are apparent. Towards SN 2001el, the strongest components are redshifted by ∼1170 km s^{-1}, while the strongest components towards SN 2003hn have a redshift of ∼1340 km s^{-1} (Fig. 3; Table 3). This is consistent with the measured heliocentric velocity of 1168 km s^{-1}, with the difference between the two positions in the galaxy reflecting the rotation velocity (∼193 km s^{-1}; Mathewson & Ford 1996).

To further analyze these line profiles we have used the program VPFIT[3] which fits multiple Voigt profiles to multiple line components. We constrained all the lines (of the same species and ionization state) to have the same width, where the theoretical line is convolved with the instrument resolution (∼6 km s^{-1}) before doing the fitting. The program adds components in an iterative way until an acceptable fit is found. This initial guess can then be adjusted interactively. The program uses a least-square fitting method to obtain the best fit, and in the end VPFIT provides velocities, widths and column densities for each line component of the ions. The obtained results are given in Table 3, and some fits performed by VPFIT are shown in Fig. 3.

[2] `www.eso.org/observing/dfo/quality/` (vers. 1.4.0 and 2.0).

[3] By R. Carswell on `www.ast.cam.ac.uk/~rfc/vpfit.html`

3.2. Diffuse Interstellar Bands

A very interesting feature of our spectra is the abundance of extragalactic DIBs. We detect more than a dozen of bands throughout the spectra of SN 2001el. A list of detected lines, identifications, observed central wavelengths ($\lambda_{\rm observed}$), velocities ($v_{\rm DIB}$), equivalent widths (EW) and Full Width Half Maxima ($FWHM$) is given in Table 4.

There are many advantages in searching for DIBs in an extragalactic supernova spectrum. All wavelengths are conveniently redshifted to avoid confusion with any MW components. In our spectra, we detect no DIBs from the MW. The strong DIB at λ 6284 is often blended with a telluric O_2 complex in the MW. Here the DIB feature is redshifted to 6308 Å, and the high resolution clearly separates the narrow telluric lines (Fig. 4). There is also no contamination from intrinsic narrow lines that needs to be modeled in the supernova spectrum, as opposed to using stars as background sources. However, the supernova spectrum is made up of a superposition of numerous broad lines. This is well suited as a quasi-continuum against which to detect narrow DIBs, but very broad DIBs are not so easy to disentangle. We have therefore not been able to clearly identify DIBs with $FWHM$ broader than ≳10 Å. For example, the usually very strong DIB at λ 4428 can not be securely identified. We emphasize that this is not to be interpreted as evidence for absence of such broad DIBs (see e.g., Ehrenfreund et al. 1997).

The sample of lines listed in Table 4 were searched among the DIBs tabulated by Herbig (1995). From this table, we have searched and detected all the strong ($EW > 200$ mÅ) lines with $FWHM < 7$ Å between 4000 and 8000 Å. The line at λ 7724 only became obvious after division with a standard star to cancel out the telluric lines. All these 9 lines have a central depth (A_c) ≳ 0.07, as defined by Herbig (1995). We therefore searched also for all the other tabulated DIBs that meet this criterion.

Apart from the broad, shallow λ 4428 feature, as discussed above, we detect also the other 4 DIBs ($\lambda\lambda$ 6196, 6379, 6661 and 6993) with $A_c \gtrsim 0.07$ in the wavelength range given above. This includes the narrow line at λ 6196, which is clearly detected. After applying the telluric correction we also detect the weak λ 6661 and λ 6993 DIBs. Six conspicious DIBs towards SN 2001el are displayed in Fig. 5. Longwards of 8000 Å, there are 3 potentially strong DIBs ($\lambda\lambda$ 8621, 9577 and 9632) according to the list of Herbig (1995), but we were unable to detect any of these lines. This region was only observed during our first epoch of observations. In this study we will use the clear detections to compare our observations with DIB observations in the MW and in other galaxies.

The spectra of SN 2003hn do not display the same multitude of DIBs as the line of sight towards SN 2001el. We were able to detect only 2 DIBs, the λ 5780 and λ 6284 with any confidence (see Table 4 and Fig. 4).

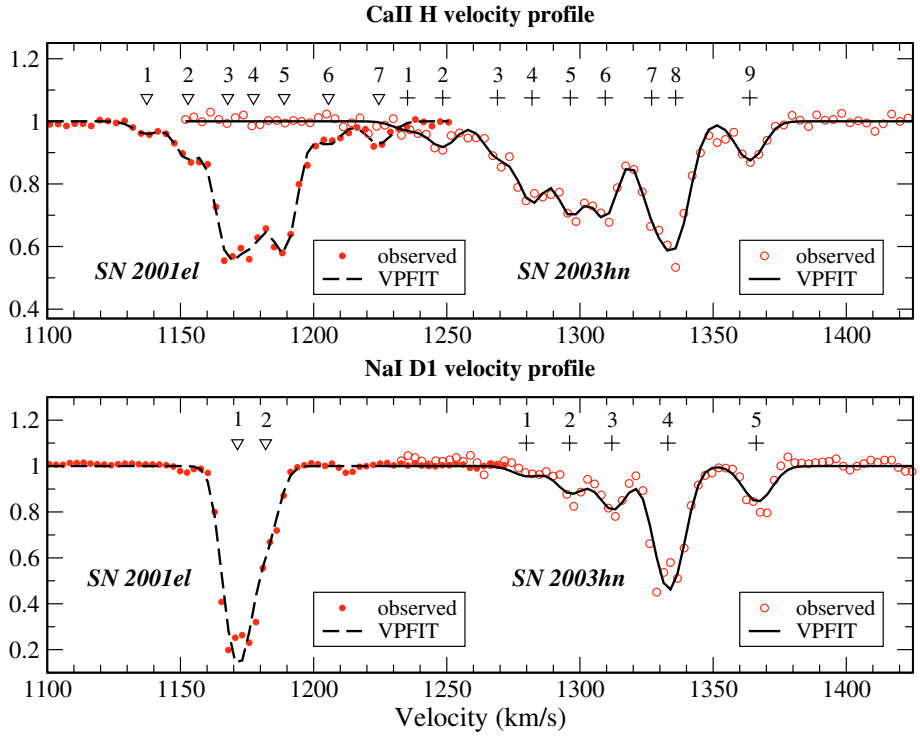

Fig. 3. Interstellar atomic lines of Ca II H (*top*) and Na I D1 (*bottom*) towards SN 2001el and SN 2003hn. The black lines (dashed for SN 2001el and solid for SN 2003hn) are the fits with VPFIT, and the grey symbols (filled dots for SN 2001el and open circles for SN 2003hn) are the observed UVES spectra. The numbered symbols (▽ for SN 2001el and + for SN 2003hn) at the top indicate the positions of the fitted velocity components. For velocities, column densities and Doppler parameters of the fit we refer to Table 3.

3.3. Extinction

There are many ways to estimate the amount of extinction towards an astronomical object. In supernova research, estimates are often made from the equivalent widths of the interstellar Na I D lines – even from low resolution spectroscopy (e.g., Turatto et al. 2003, and references therein). In this work we have high quality high resolution spectra and are able to deduce the actual column densities for these lines. Moreover, for Type Ia supernovae, an estimate of the reddening can be directly obtained from the supernova colors. Therefore, this dataset allows a comparison between the different methods.

3.3.1. Equivalent width and column densities

The use of the Na I D EW to estimate the amount of reddening (e.g., Barbon et al. 1990; Turatto et al. 2003) often assumes that the effects of saturation are negligible. However, this is not valid for our observations. Table 5 shows our measurements of the *EW* and column densities towards the two SNe.

In this table we have first assumed an optically thin line for which the column density is directly proportional to the equivalent width (e.g., Spitzer 1978). In the lower part of this table we also show the results from the so called doublet ratio (DR) technique (e.g., Somerville 1988), as well as the total column densities derived with VPFIT. It is clear that the optically thin approximation is not valid for the saturated doublet lines towards NGC 1448. Taking the saturation into account via either the DR method or the component fitting procedure (VPFIT) gives column densities that are mutually consistent. A simple Na I D EW approach to estimate the amount of reddening towards a supernova can thus give substantial errors (see also discussions by e.g., Munari & Zwitter 1997; Fassia et al. 2000; Smartt et al. 2002). We will use the column densities derived by VPFIT to estimate the amount of reddening below.

3.3.2. Estimate of $E(B-V)$

Adopting the relation from Hobbs (1974) we can use our measured sodium column densities to directly derive the reddenings towards the supernovae. This gives $E(B-V)_{\rm host} = 0.15$ and 0.12 mag for SN 2001el and SN 2003hn, respectively. The values for the MW components are $E(B-V)_{\rm MW} = 0.021$ and 0.017 mag, respectively. For the MW components we can directly compare this to the value derived by Schlegel et al. (1998), $E(B-V)_{\rm MW} = 0.014$ mag.

Alternatively (following e.g., Fassia et al. 2000), one can convert the sodium column density to hydrogen column density (Ferlet et al. 1985) assuming a MW gas-to-dust ratio, and then derive the color excess (Bohlin et al. 1978). This gives $E(B-V)_{\rm host} = 0.18$ mag towards SN 2001el.

Another way to measure the reddening towards SN 2001el is from the supernova light curve itself. It has been established that Type Ia supernovae display a uniform intrinsic color evolution from 30 to 90 days past maximum (Lira 1995; Phillips et al. 1999). The light curve of SN 2001el has been very well monitored by Krisciunas et al. (2003). They

Table 4. DIBs in NGC 1448 towards SNe 2001el and 2003hn. Central velocities were derived by fitting high resolution DIB profiles of single cloud galactic lines of sight to the observed DIBs profiles.

DIB	NGC 1448				Average [c]	HD 144217[d]	HD 149757[d]	LMC [e]	SN 1986G [f]
λ_{rest} [a] (Å)	$\lambda_{observed}$ (Å)	v_{DIB} (km s^{-1})	*EW* (mÅ)	*FWHM* (Å)	EW_{scaled} (mÅ)	*EW* (mÅ)	*EW* (mÅ)	*EW* (mÅ)	*EW* (mÅ)
SN 2001el:									
5705.20	5727.55	1174.4 ± 21.0	37 ± 5	2.23	17	93	–	20 ± 9	79 ± 5
5780.37	5802.97	1172.1 ± 5.2	189 ± 3	2.04	104	160	66	145 ± 21	335 ± 5
5796.97	5819.67	1173.9 ± 3.9	26 ± 2	0.75	24	22	27	28 ± 6	151 ± 5
6195.97	6220.17	1170.9 ± 4.8	15 ± 2	0.37	11	20	10	10 ± 3	30 ± 15
6203.08[b]	6227.28	1169.6 ± 9.7	26 ± 3	1.35	19	} 66	11	50 ± 20	191 ± 5
6204.66[b]	6228.50	1151.9 ± 9.7	76 ± 4	4.6	34		18	included in 6203	
6269.75	6294.15	1166.7 ± 14.3	35 ± 8	1.65	14	23	10	4 ± 8	–
6283.85[g]	6308.25	1164.1 ± 23.8	500 ± 80	2.5	111	390	111	225 ± 21	–
6379.29	6404.19	1170.2 ± 4.5	12 ± 3	0.48	14	14	24	55 ± 14	75 ± 8
6613.56	6639.36	1169.5 ± 4.1	52 ± 3	1.00	42	40	43	19 ± 6	–
6660.64	6686.77	1176.1 ± 4.6	13 ± 5	0.70	9	–	–	–	–
6993.18	7020.58	1166.9 ± 4.9	23 ± 7	0.79	21	–	–	–	–
7223.96	7251.96	1162.0 ± 4.1	74 ± 5	0.90	47	–	–	–	–
SN 2003hn:									
5780.37	5805.3	1293.0 ± 40	52 ± 7	2.4					
6283.85	6311.9	1338.2 ± 52	130 ± 11	5.0					

[a] Included are DIBs with $A_c \gtrsim 0.07$ from the table of Herbig (1995). Rest wavelengths from the Galazutdinov et al. (2000) survey.
[b] The 6203.10 and 6204.27 DIBs are two partly overlapping DIBs, which are sometimes taken to be a single DIB feature.
[c] DIB equivalent width for the MW "average diffuse cloud" (Jenniskens & Desert 1994) scaled to $E(B-V) = 0.18$ mag, i.e. that within the host galaxy towards SN 2001el.
[d] Galactic lines of sight with $E(B-V) = 0.20$ and 0.32 mag for HD 144217 and HD 149757, respectively. Data from FEROS program 64.H-0224 obtained by one of us (LK).
[e] Values for Sk-69 223, $E(B-V) \approx 0.35$ mag, from Cox et al. (in preparation).
[f] From D'Odorico et al. (1989). Note revised $E(B-V) = 0.6$ mag (Nugent et al. 2002). The equivalent width given for λ 6203 includes also the λ 6204 DIB, and the λ 6379 DIB equivalent width includes the λ 6376 DIB.
[g] The *FWHM* applies to the strong "narrow" component of the 6284 Å DIB. The *EW* includes the broader underlying component.

obtained various estimates of the color excess using the intrinsic color of the supernova. Using the light curve tail, a value of $E(B-V)_{total} = 0.253 \pm 0.063$ mag is reported, whereas an average of all the six different methods used by Krisciunas et al. gives $E(B-V)_{total} = 0.185 \pm 0.07$ mag. Here the error is a combination of the propagated errors of the different estimates and the standard deviation in the estimates themselves. When we compare this with the total reddening towards SN 2001el derived from the sodium lines, we find a good agreement within the errors. Below we will use $E(B-V)_{host} = 0.18 \pm 0.08$ mag for SN 2001el. This value encapsulates most of the estimates given in this section.

4. Discussion

4.1. Line profiles

In Fig. 5 we show the line profiles of several conspicuous DIBs in NGC 1448. The spectra are shown in velocity scale in kilometers per second with respect to the central wavelength indicated in the figure.

The λ 6613 line exhibits a much steeper blue side of the profile, and this can also be perceived, for example, in the λ 5797 line. The $\lambda\lambda$ 6284 and 5780 DIBs have quite similar line profiles, and are clearly not simple Gaussians. The observed profiles actually show a strong resemblance to those seen towards galactic single cloud lines of sight. To illustrate this we also show two typical galactic lines of sight that represent the so called σ (HD 144217) and ζ (HD 149757) type diffuse clouds (see e.g., Krelowski & Sneden 1995). These galactic spectra were obtained with the FEROS instrument by one of us (LK). These lines of sight have $E(B-V)$ of 0.20 mag and 0.32 mag, respectively. Note that the SN 2001el DIBs show the same asymmetries in the profiles as the MW DIBs.

4.2. DIB velocities

In Fig. 6 we explore the link between DIB velocities and atomic line velocities. It is clear that the DIB carriers (of the narrow DIBs) are, in velocity, closely related to the strongest Ca II and Na I line components. The four narrowest DIBs ($\lambda\lambda$ 6379, 6613, 6661 and 6993) have well determined central velocities

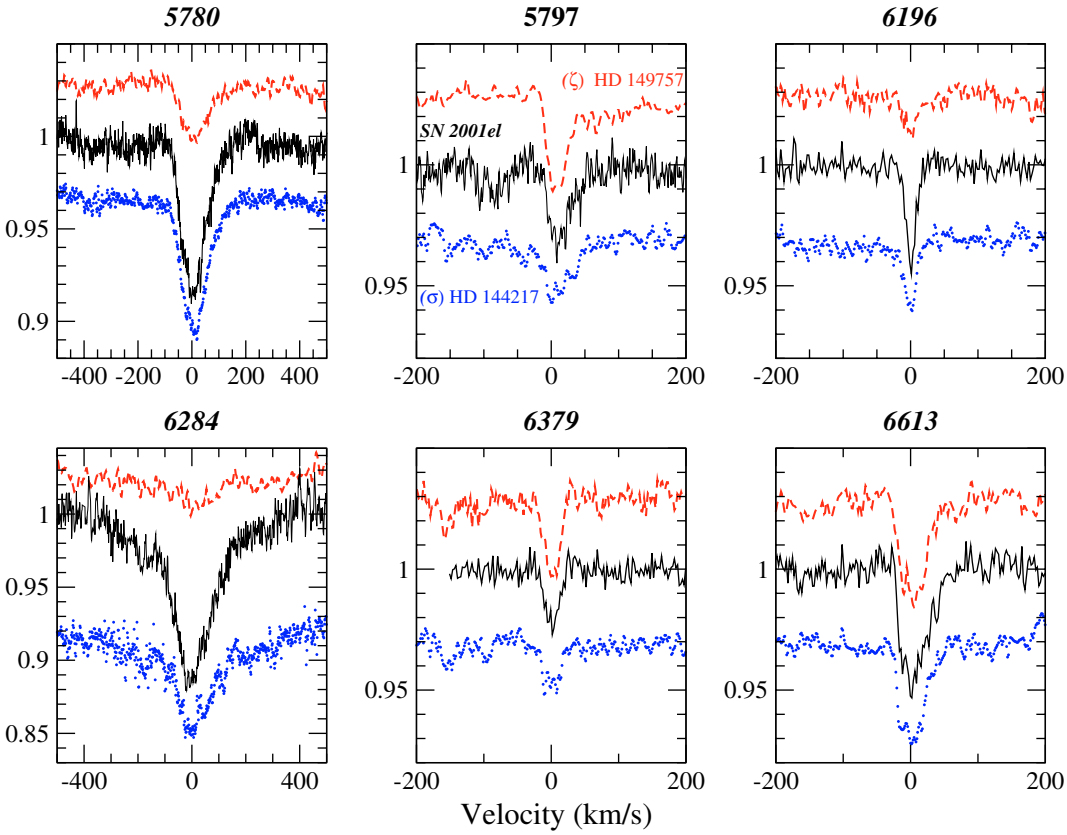

Fig. 5. The six panels show, on a velocity scale centered on the DIBs, some of the most important and well studied DIBs ($\lambda\lambda$ 5780, 5797, 6196, 6284, 6379 and λ 6613) as observed towards SN 2001el. Overplotted are the observed FEROS DIB spectra towards the ζ type cloud in the line of sight to HD 149757 (*top*, $E(B-V) = 0.32$ mag) and the σ type cloud HD 144217 (*bottom*, $E(B-V) = 0.20$ mag). These spectra are not scaled, but shifted vertically for clarity. For measured values of the DIB velocities, equivalent widths and full-width half maxima see Table 4.

Table 5. The column densities towards SNe 2001el and 2003hn derived by different methods. The upper panel values are derived from the *EW* and an optically thin approximation ignoring the effects of saturation (see text). The lowermost panel shows instead the values derived via the doublet ratio (DR) technique (i.e., curve of growth technique applied to doublet lines), as well as the total column densities derived with VPFIT. The optically thin approximation is not valid for the saturated doublet lines towards NGC 1448, giving values that underestimate the true column density.

Supernovae in NGC 1448: Interstellar Atomic Lines					
		SN 2001el		SN 2003hn	
Line		*EW* (mÅ)	log *N* (cm^{-2})	*EW* (mÅ)	log *N* (cm^{-2})
Ca II K	MW	104(1)	12.04	104(4)	12.04
	NGC	366(2)	12.59	525(6)	12.75
Ca II H	MW	54(1)	12.06	60(6)	12.10
	NGC	220(1)	12.67	320(7)	12.83
Na I D2	MW	37(1)	11.27	35(4)	11.25
	NGC	367(2)	12.27	503(5)	12.41
Na I D1	MW	–	–	–	–
	NGC	302(2)	12.49	289(7)	12.47
		Column density log *N* (cm^{-2})			
Line		DR	VPFIT	DR	VPFIT
Ca II	MW	$12.07^{+0.02}_{-0.02}$	12.12 ± 0.05	$12.17^{+0.12}_{-0.11}$	12.12 ± 0.14
	NGC	$12.76^{+0.04}_{-0.05}$	12.79 ± 0.08	$12.93^{+0.17}_{-0.18}$	12.89 ± 0.20
Na I	NGC	$12.88^{+0.03}_{-0.03}$	12.76 ± 0.04	$12.52^{+0.03}_{-0.02}$	12.55 ± 0.09

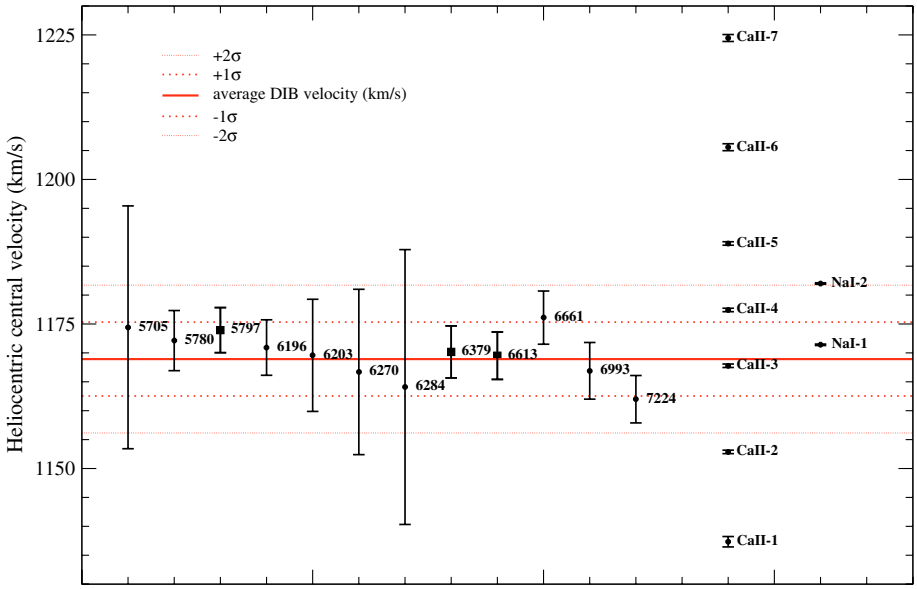

Fig. 6. The central heliocentric velocities of the DIBs observed towards SN 2001el. The square symbols indicate the λ5797, λ6379 and λ6613 family (Cami et al. 1997). The derived velocities of the individual Ca II and Na I components are also indicated. The central velocities for the strong, narrow DIBs are well defined, whereas those of the broader and/or weaker are less stringent. The average DIB velocity coincides with the strongest interstellar line components Ca II-3 and Na I-1, and within 2σ also with the components Ca II-4 and Na I-2. Although these two component-pairs have very similar column densities (and corresponding N(Na I)/N(Ca II) ratios), one velocity component seems to be favoured by the DIBs. The SN 2001el DIBs (Table 4) show no broadening with respect to the single cloud lines of sight (Fig. 5), and might thus be expected to originate within a small velocity range.

that can be assigned, within the errors, to components 3 and 1 of the Ca II and Na I profiles, respectively. This velocity coincidence indicates that the carriers of these DIBs are physically associated, and probably located within the same cloud in NGC 1448.

Since we also observe no broadening of the profiles with respect to the single cloud DIBs towards HD 144217 and HD 149757 (Fig. 5) we conclude that the DIBs towards SN 2001el primarily form in a single gas-rich layer, indicated by these strong absorption components of ionized Ca and neutral Na.

4.3. DIB ratios

Two potentially important DIBs for the determination of the ionization balance are the ones at λ5797 and λ5780. According to Cami et al. (1997) the λ5780 DIB has a higher ionization potential than the λ5797 DIB, and thus reaches its maximum only with a stronger UV field. For SN 2001el the λ5780 DIB is very strong compared to the λ5797 DIB. This behavior is indicative of a so called σ type cloud like environment (Fig. 5). In such a cloud Ca I and simple interstellar molecules (CH, CN) are very weak or undetectable. This is also true for our observations, where the 3σ upper limits on CH, CN are 7 and 10 mÅ, respectively.

From Table 4 we can compare the 5797/5780 ratio for different galactic and extragalactic targets. The denser single cloud towards HD 149757 has a relatively high ratio (~0.4), while for NGC 1448, the LMC and HD 144217 we see ratios of about 0.15, which within the interpretation of Cami et al. (1997) indicate a somewhat higher UV field.

4.4. Extragalactic DIBs

As mentioned in the introduction, extragalactic DIBs have only been observed in a few cases. In this study the quality of the data allows a detailed comparison with the DIBs in the Milky Way.

For SN 2001el we compare all the DIBs with an "average cloud" in the MW as given in Table 4. Although the DIBs against SN 2001el appear relatively strong, this could just be due to the uncertainty in the determination of the reddening. The DIB strengths would be similar to those of the average cloud for an $E(B-V) \sim 0.3$ mag, which is still within the error budget.

In fact, as illustrated in Fig. 5 and given in Table 4, we find that the properties of the DIBs in NGC 1448 closely mimic those observed towards HD 144217. Both the line profiles and the relative strengths are similar for these lines of sight, illustrating the potential for studying how DIB carriers behave in different extragalactic environments. It could also indicate that very similar local environmental conditions pretain in those different lines of sight.

We have also compiled a sample of extragalactic DIBs to compare with the properties of the MW DIBs. In Fig. 7 we extend the exercise of Heckman & Lehnert (2000) and plot the EW of the $\lambda\lambda$5780 and 6284 DIBs versus the total sodium column density. The extragalactic sight lines show, for their respective reddenings, similar EWs compared to the galactic average. In the left panel we have not included the detections classified as tentative by Heckman & Lehnert (2000). These would appear significantly below the fitted line.

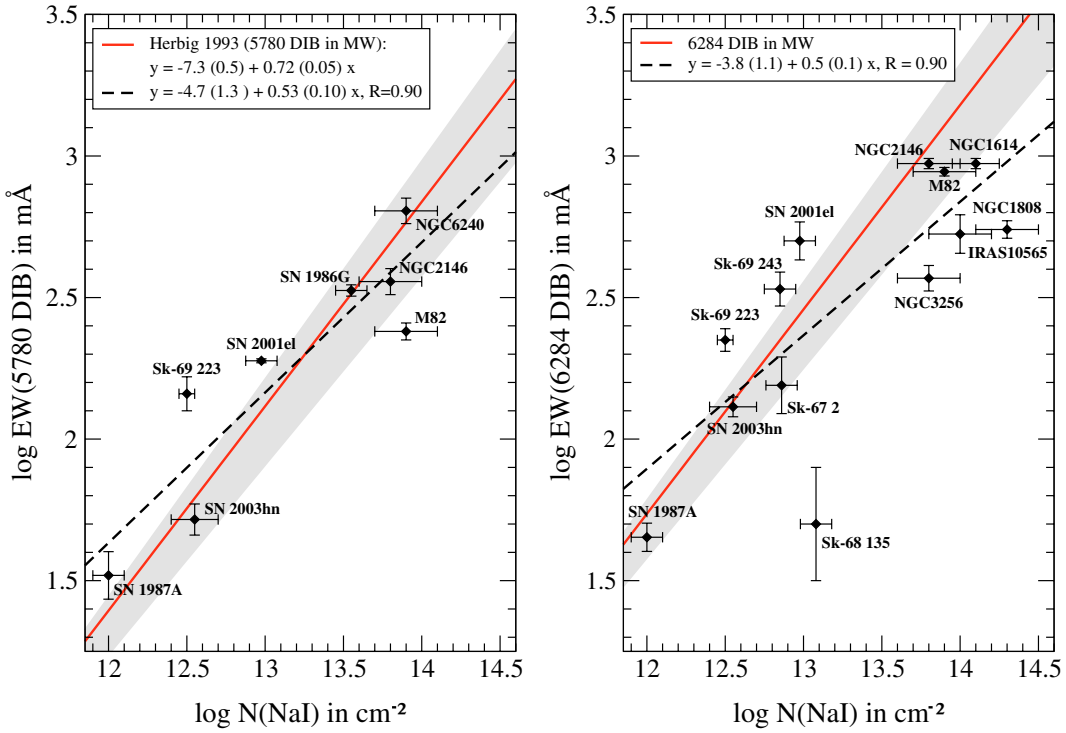

Fig. 7. The equivalent widths of the extragalactic DIBs λ 5780 (*left panel*) and λ 6284 (*right panel*) are plotted versus the extragalactic Na I column densities in their line-of-sights. Total column densities have been derived from the Na I line and do not take into account individual components. SN 1987A data are from Vladilo et al. (1987) and Vidal-Majar et al. (1987). Sk-69 223 (LMC) data are from Cox et al. (in preparation), and Sk-67 2, Sk-68 135 from Ehrenfreund et al. (2002). SN 1986G data are from D'Odorico et al. (1989). The remaining extragalactic points are starburst galaxies from Heckman & Lehnert (2000). The solid line in the left panel is the relationship from Herbig (1993) for the MW. The grey region illustrates the 1σ uncertainty region for that relation. In the right panel, this relationship has been converted for the λ 6284 DIB assuming $\langle 5780/6284 \rangle = 2.2$, as done in Heckman & Lehnert (2000). The dashed lines are the best linear fits to the extragalactic data.

Herbig (1995) summarized that extragalactic DIBs did not show conclusive evidence for any variation of DIB strengths versus color excess, partly due to the large scatter in the Galactic data. This seems to hold also for the data presented here.

4.5. Location of the absorbing gas

The information we have gathered could potentially provide some clues on the location and origin of the material in which the DIBs are produced. It may even be of interest to investigate to which extent this material is physically connected to the local supernova environment.

Jenkins et al. (1984) noted for SN 1983N that the presence of neutral sodium and singly ionized calcium argue against absorbing gas close to the supernova location. Since towards SN 2001el these ISM lines are correlated with the DIBs (Fig. 6) the same argument would imply that the DIBs are not directly located in the supernova environment. Also, we measure no variability in the DIBs between the two epochs (e.g., the *EW* for the λ 6613 DIB is stable to about 6%). This does not favor a scenario were the DIBs are produced in gas closely associated with the supernova itself, and is consistent with conclusions from supernovae Type Ia investigations arguing that the dust dimming the supernovae is generally interstellar rather than circumstellar (e.g., Riess et al. 1996).

The ToO programme behind these data has also observed a few other supernovae of various types; SN 2000cx (type Ia), SN 2001ig (IIb), SN 2003bg (II). None of these showed any signatures (>2σ) of the strongest DIBs ($\lambda\lambda$ 5780, 6284). SN 2000cx and SN 2001ig would have revealed bands similar in strength to those seen towards SN 2003hn. In the noisier spectrum of SN 2003bg we would only have detected (~2σ) bands as strong as those seen towards SN 2001el.

For the other supernovae where DIBs have been seen (SN 1986G, SN 1987A, SN 1989M) there is also no clear correlation between the DIB strengths and the supernova type.

To truly compare the different supernova sight lines would require a more thorough investigation of the host galaxies, including for example their metallicities. This is beyond the scope of this investigation – where the main aim was instead to demonstrate the potential of probing DIBs in external galaxies using supernovae as transitory luminous probes for high resolution spectroscopy.

5. Conclusions

Using high resolution spectroscopy of two emerging supernovae in NGC 1448 we have detected a number of extragalactic atomic interstellar lines. Towards SN 2001el we also detected a large number of Diffuse Interstellar Bands.

We have compared the properties of the DIBs in NGC 1448 with those of the DIBs observed both in our own Galaxy and

in other galaxies. These observations probe the most distant system where a larger number of DIBs has been analyzed in such a detail. These DIBs show many similarities with DIBs within the Milky Way, especially with those seen towards the σ-type cloud HD 144217. This shows the potential for modern telescopes to investigate how DIB carriers follow common chemical and physical pathways throughout the universe.

We have shown that the DIBs towards SN 2001el are associated in velocity space with specific components of the atomic interstellar lines. We observe no DIB strength time variability on time scales shorter than a week, nor do we see any direct connection between DIB properties and supernova type.

We have also probed the extinction towards the supernovae in several different ways. Taking the saturation of the interstellar sodium lines into account in our high-resolution data gives a reddening estimate consistent with color excess measurements from the Type Ia SN 2001el itself.

Acknowledgements. These observations were obtained in ToO service mode at the VLT. We wish to thank the Paranal staff for all the help. We also thank J. Fynbo for comments on the manuscript. C. Fransson, E. Baron and K. Nomoto were helpful in writing the original UVES proposals. NC acknowledges NOVA for financial support and SM acknowledges financial support from the "Physics of Type Ia SNe" RTN.

References

Barbon, R., Benetti, S., Rosino, L., Cappellaro, E., & Turatto, M. 1990, A&A, 237, 79
Bohlin, R. C., Savage, B. D., & Drake, J. F. 1978, ApJ, 224, 132
Cami, J., Sonnentrucker, P., Ehrenfreund, P., & Foing, B. H. 1997, A&A, 326, 822
D'Odorico, S., di Serego Alighieri, S., Pettini, M., et al. 1989, A&A, 215, 21
Ehrenfreund, P., Cami, J., Dartois, E., & Foing, B. H. 1997, A&A, 317, L28
Ehrenfreund, P., Cami, J., Jiménez-Vicente, J., et al. 2002, ApJ, 576, 117
Evans, R. 2003, IAUC, 8186
Fassia, A., Meikle, W. P. S., Vacca, W. D., et al. 2000, MNRAS, 318, 1093
Ferlet, R., Vidal-Madjar, A., & Gry, C. 1985, ApJ, 298, 838
Galazutdinov, G. A., Musaev, F. A., Krełowski, J., & Walker, G. A. H. 2000, PASP, 112, 648
Heckman, T. M., & Lehnert, M. D. 2000, ApJ, 537, 690
Herbig, G. H. 1995, ARA&A, 33, 19
Hobbs, L. M. 1974, ApJ, 191, 381
Jenkins, E. B., Rodgers, A. W., Harding, P., Morton, D. C., & York, D. G. 1984, ApJ, 281, 585
Jenniskens, P., & Desert, F.-X. 1994, A&AS, 106, 39
Kaufer, A., D'Odorico, S., & Kaper, L. 2002, UVES manual
Krełowski, J., & Sneden, C. 1995, in Diffuse Interstellar Bands, ed. Tielens & Snow (Kluwer Academic Publisher), 13
Krisciunas, K., Suntzeff, N. B., Candia, P., et al. 2003, AJ, 125, 166
Lira, P. 1995, Masters thesis, Univ. Chile
Lundqvist, P., Mattila, S., Sollerman, J., et al. 2004, To appear in Proceedings "Supernovae", IAU Coll., 192, ed. J. M. Marcaide, & K. W. Weiler [arXiv:astro-ph/0309006]
Mathewson, D. S., & Ford, V. L. 1996, ApJS, 107, 97
Monard, A. G. 2001, IAUC, 7721
Morgan, D. H. 1987, QJRAS, 28, 328
Munari, U., & Zwitter, T. 1997, A&A, 318, 269
Nugent, P., Kim, A., & Perlmutter, S. 2002, PASP, 114, 803
Phillips, M. M., Lira, P., Suntzeff, N. B., et al. 1999, AJ, 118, 1766
Rich, M. R. 1987, AJ, 94, 651
Riess, A. G., Press, W. H., & Kirshner, R. P. 1996, ApJ, 473, 588
Salvo, M., Bessel, M., & Schmidt, B. 2003, IAUC, 8187
Schlegel, D. J., Finkbeiner, D. P., & Davis, M. 1998, ApJ, 500, 525
Smartt, S., Gilmore, G. F., Tout, C. A., & Hodgkin, S. T. 2002, ApJ, 565, 1089
Sollerman, J., Leibundgut, B., & Lundqvist, P. 2001, IAUC, 7723
Somerville, W. B. 1988, The Observatory, 108, 44
Spitzer, L. 1978, Physical processes in the interstellar medium (Interscience: New York Wiley)
Steidel, C. C., Rich, R. M., & McCarthy, J. K. 1990, AJ, 99, 1476
Turatto, M., Benetti, S., & Cappellaro, E. 2003, in From Twilight to Highlight – The Physics of Supernovae, Ed. W. Hillebrandt, & B. Leibundgut, 200 [arXiv:astro-ph/0211219]
Vidal-Madjar, A., Andreani, P., Cristiani, S., et al. 1987, A&A, 177, 17
Vladilo, G., Crivellari, L., Molaro, P., & Beckman, J. E. 1987, A&A, 182, 59
Voung, M. H., & Foing, B. H. 2000, A&A, 363, 5

Online Material

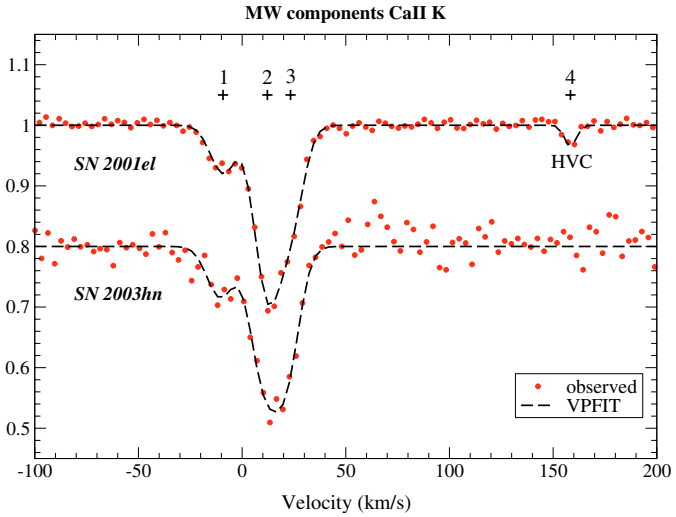

Fig. 2. Interstellar atomic Milky Way components of Ca II K in the line-of-sight towards SN 2001el and SN 2003hn. The black dashed lines refer to the fits by VPFIT, and the grey dots to the observed UVES spectra. For velocities, column densities and Doppler parameters of the fits we refer to Table 3. The numbered symbols (+) at the top indicate the positions of the fitted velocity components. The lower spectrum has been displaced vertically for clarity. A high velocity cloud at ∼160 km s^{-1} can also be seen towards SN 2001el (component 4).

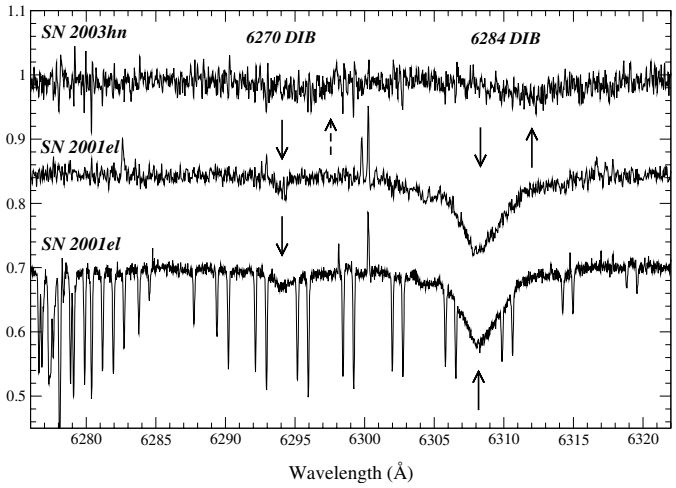

Fig. 4. The λ 6284 DIB towards SN 2001el is redshifted to 6308 Å and is clearly separated from the narrow telluric O_2 complex at ∼6278 Å (*bottom*). Note also the λ 6270 DIB at 6294 Å. For illustrative purposes we show both the telluric uncorrected and corrected λ 6284 DIB for SN 2001el (*bottom and middle*). These spectra have been displaced vertically for clarity. For SN 2003hn only the telluric corrected spectrum is shown (*top*). In this sight line we detect the λ 6284 DIB at λ 6312.

Table 3. VPFIT parameters (velocity v, Doppler parameter b and column density N) for the components of the observed atomic interstellar lines of Ca II, Ti II, Na I and K I towards SN 2001el and SN 2003hn. In the last column we give the total column density, summed over the individual components.

	Line[a]	Component	v (km s^{-1})	b^b (km s^{-1})	log N (cm^{-2})	Total log N (cm^{-2})
MW components:						
SN 2001el	Ca II	1	23.3 ± 0.3	7.6 ± 0.3	11.57 ± 0.03	
	Ca II	2	12.2 ± 0.3		11.86 ± 0.02	12.12 ± 0.03
	Ca II	3	–9.2 ± 0.6		11.28 ± 0.02	
	Ca II	4	158.4 ± 1.2	1.7 ± 4.1	10.60 ± 0.08	10.60 ± 0.08
	Ti II	1	11.2 ± 12.0	9.7 ± 7.3	11.59 ± 0.63	11.83 ± 0.50
	Ti II	2	21.4 ± 8.1		11.45 ± 0.82	
	Na I	1	17.2 ± 0.6	10.1 ± 1.0	11.21 ± 0.03	11.21 ± 0.03
SN 2003hn	Ca II	1	20.74 ± 1.2	8.0 ± 1.3	11.75 ± 0.09	
	Ca II	2	10.0 ± 1.8		11.73 ± 0.09	12.12 ± 0.06
	Ca II	3	–10.7 ± 1.8		11.32 ± 0.07	
	Na I	1	19.3 ± 1.2	5.9 ± 1.9	11.04 ± 0.08	11.04 ± 0.08
NGC 1448 components:						
SN 2001el	Ca II	1	1137.3 ± 0.9	5.3 ± 0.2	11.08 ± 0.06	
	Ca II	2	1152.9 ± 0.3		11.64 ± 0.02	
	Ca II	3	1167.8 ± 0.3		12.26 ± 0.02	
	Ca II	4	1177.4 ± 0.3		12.17 ± 0.02	12.79 ± 0.01
	Ca II	5	1188.9 ± 0.3		12.26 ± 0.01	
	Ca II	6	1205.6 ± 0.6		11.38 ± 0.03	
	Ca II	7	1224.5 ± 0.6		11.33 ± 0.03	
	Na I	1	1171.4 ± 0.1	5.0 ± 0.2	12.68 ± 0.03	12.76 ± 0.03
	Na I	2	1182.0 ± 0.1		11.96 ± 0.03	
	Ti II	1	1148.0 ± 3.6	12.9 ± 3.4	11.78 ± 0.11	
	Ti II	2	1174.7 ± 25.5		12.40 ± 1.98	12.69 ± 1.40
	Ti II	3	1181.6 ± 18.6		12.15 ± 3.42	
	Ti II	4	1203.1 ± 6.9		11.64 ± 0.32	
	K I	1	1166.6 ± 0.6	1.4 ± 0.9	11.02 ± 0.07	11.29 ± 0.05
	K I	2	1175.6 ± 0.6		10.96 ± 0.06	
SN 2003hn:	Ca II	1	1235.3 ± 3.6	6.9 ± 0.5	11.08 ± 0.16	
	Ca II	2	1248.5 ± 1.5		11.42 ± 0.08	
	Ca II	3	1269.0 ± 1.5		11.70 ± 0.07	
	Ca II	4	1282.0 ± 0.9		12.03 ± 0.04	
	Ca II	5	1296.4 ± 0.9		12.14 ± 0.03	12.89 ± 0.03
	Ca II	6	1309.5 ± 0.6		12.14 ± 0.03	
	Ca II	7	1326.9 ± 1.5		12.17 ± 0.11	
	Ca II	8	1335.9 ± 0.9		12.06 ± 0.12	
	Ca II	9	1363.8 ± 0.6		11.64 ± 0.04	
	Na I	1	1279.9 ± 1.5	6.4 ± 0.2	11.08 ± 0.08	
	Na I	2	1296.1 ± 0.6		11.53 ± 0.03	
	Na I	3	1312.0 ± 0.3		11.75 ± 0.02	12.55 ± 0.01
	Na I	4	1333.0 ± 0.3		12.32 ± 0.01	
	Na I	5	1366.2 ± 0.3		11.65 ± 0.02	
	Ti II	1	1281.7 ± 0.9	6.8 ± 0.8	12.17 ± 0.06	
	Ti II	2	1293.4 ± 1.5		11.84 ± 0.11	12.64 ± 0.04
	Ti II	3	1324.6 ± 1.2		12.01 ± 0.07	
	Ti II	4	1337.5 ± 0.9		12.07 ± 0.06	

[a] We use the doublet lines of Ca II, Na I and K I to constrain the least square fitting routine employed by VPFIT.
[b] The doppler parameter, b, has for each atomic line been set equal for all components.